



## Letter

## Influence of texture on strain localization in stir zone of friction stir welded titanium

F.C. Liu <sup>a,\*</sup>, J. Liao <sup>b</sup>, Y. Gao <sup>a</sup>, K. Nakata <sup>a</sup><sup>a</sup>JWRI, Osaka University, 11-1 Mihigaoka, Ibaraki, Osaka 567-0047, Japan<sup>b</sup>Kurimoto Ltd, 2-8-45 Suminoe, Osaka 559-0021, Japan

## ARTICLE INFO

## Article history:

Received 17 September 2014

Received in revised form 5 November 2014

Accepted 3 December 2014

Available online 12 December 2014

## Keywords:

Joining

Titanium

Texture

Prismatic slip

Twining

Strain localization

## ABSTRACT

Friction stir welding has a great advantage in welding of titanium because it can avoid solidification problems and generate fine grain structure in the weld region. However, the strong texture formed in the weld region may affect the mechanical properties and deformation behavior of the joints. The present work seeks to understand the comprehensive effect of grain structure and texture on the local deformation behavior in the weld region. It was found that although the weld region had a finer grain structure and a higher hardness than the base material (BM), a distinctive plastic deformation extensively occurred within the weld region during the initial tensile deformation stage because the Schmid factor for prismatic slip in the weld region is much higher than that in the BM. At high strain, the difference of Schmid factor for prismatic slip deformation between the weld region and the BM was significantly reduced and the effect of grain size became more significant than Schmid factor. Therefore, the local deformation in the weld region was restrained, and the tensile sample failed in the BM finally.

© 2014 Elsevier B.V. All rights reserved.

## 1. Introduction

With increasing the utilization of commercially pure (CP) Ti in the chemical and aerospace industries due to its extremely excellent corrosion resistance, the welding issues of this alloy need to be addressed urgently [1,2]. Fusion welding of CP Ti is not recommended because the joints usually associate with weld embrittlement, high residual stresses and distortion due to the low thermal conductivity of titanium [2]. As a solid-state process, friction stir welding (FSW) has received much attention in joining CP Ti due to the avoidance of solidification problems associated with conventional fusion welding [3–7]. After FSW, the grains of CP Ti in the stir zone (SZ) were significantly refined [8,9], which is generally estimated to be beneficial for the improvement of strength and ductility.

For hexagonal close-packed CP Ti, prismatic slip  $\{10\bar{1}0\}\langle 1\bar{2}10\rangle$  is the dominant deformation mode [9,10]. The prismatic slip occurs when the resolved shear stress  $\tau_R$  acting in the slip direction  $\langle 1\bar{2}10\rangle$  on the slip plane  $\{10\bar{1}0\}$  reaches a critical value, i.e. the critical resolved shear stress  $\tau_C$ . The  $\tau_R$  can be calculated using following formula.

$$\tau_R = \sigma \cos \phi \cos \lambda \quad (1)$$

where  $\sigma$  is the applied stress during tensile test,  $\phi$  is the angle between tensile direction and normal direction of slip plane  $\{10\bar{1}0\}$ , and  $\lambda$  is the angle between the tensile direction and slip direction  $\langle 1\bar{2}10\rangle$ . If the  $\cos \phi \cos \lambda$ , which is known as the Schmid factor, is larger, the deformation is easier.

It has been accepted that [9–12] the materials flow during FSW of CP Ti arose from the simple shear deformation (the shear surface being roughly around the stir tool), resulting in the formation of P-fiber simple shear texture in the SZ which is associated with predominance of the prismatic  $\{10\bar{1}0\}\langle 1\bar{2}10\rangle$  slip with some contribution of basal  $\{0001\}\langle 1\bar{2}10\rangle$  and pyramidal  $\{10\bar{1}1\}\langle 1\bar{2}10\rangle$  slips. Such a strong texture formed in the SZ may cause high Schmid factor for prismatic slip under tensile stress, which may induce strain localization in the SZ or reduce the deformation resistance of the FSW CP Ti joints.

The grain refinement and texture may have contrary effects on the deformation resistance in the SZ. To the best of our knowledge, all the published research works only clarified the grain structural development and textural formation during FSW of CP Ti [8–12], but the specific investigation about how the obtained grain structure and texture affect the local deformation in the SZ has not been reported. In this study, CP Ti sheets were butt welded using FSW and then were subjected to tensile test and microstructural examination for the purpose of understanding the comprehensive influence of texture and grain structure on the strain localization in the SZ.

\* Corresponding author. Tel.: +81 6 68798668; fax: +81 6 68798658.

E-mail address: [fcgliu@alum.imr.ac.cn](mailto:fcgliu@alum.imr.ac.cn) (F.C. Liu).

## 2. Experimental

The CP Ti sheets with dimensions of  $300 \times 100 \times 2$  mm were used, and this alloy had a chemical composition of Ti-0.01 C-0.03 Fe-0.01 N-0.1 O-0.001 H (in wt.%). The butt welding of two plates through FSW was carried out under plunge depth control using a sintered WC-Co tool (tilted at  $3^\circ$  from the vertical) consisting of a shoulder of 15 mm in diameter, a probe 6 mm in diameter and 1.9 mm in length. The rotation rate was varied from 250 to 400 rpm and the welding speed was varied from 50 to 150 mm/min. The water cooling and argon shielding systems were utilized to cool the welding tool and minimize surface oxidation, respectively.

After welding, the FSW samples were cross-sectioned perpendicular to the welding direction for microstructural examination and mechanical properties testing. The cross-sections were mechanical polished and then were etched in a solution comprising of hydrofluoric acid, nitric acid and distilled water at a volume ratio of 1:1:8 to reveal the microstructures in these samples. Finally, the specimens were observed by an optical microscope (VHX; Keyence Corp). The samples for electron back scattered diffraction (EBSD) examination were prepared using an ion polisher (JEOL SM-09010) and were analyzed using a scanning electron microscope (JSM-6400; JEOL Ltd.) equipped with a MSC-2200 orientation imaging microscopy system (TexSEM Laboratories).

Microhardness measurements were made across the weld zone at the middle thickness of the plate cross sections using a Mitutoyo MicroWizhard hardness testing machine under a load of 0.98 N for 15 s. Tensile specimens with a gage length of 100 mm, a width of 12 mm were cut from the FSW joints with the tensile direction vertical to the welding direction. The top and bottom surfaces of the tensile samples were removed symmetrically to eliminate the rough surfaces, and the final thickness of the tensile samples was 1.2 mm. All the tests were performed at a strain rate of  $1 \times 10^{-3} \text{ s}^{-1}$ . At least six specimens were tested for each condition. The changes in width and thickness were measured on the tensile specimens around BM and SZ regions. The local elongation in the BM and SZ was calculated according to the law of volume constancy. Normal anisotropy ratio ( $r$ ) were calculated in each specimen as

$$r = \Phi_w / \Phi_t \quad (2)$$

where  $\Phi_w$  and  $\Phi_t$  are the true plastic strain along the specimen width  $w$  and thickness  $t$ , respectively. For the FSP specimen,  $\Phi_w$  and  $\Phi_t$  are estimated respectively by

$$\Phi_w = 1/4(\Phi_{wt} + 2\Phi_{wm} + \Phi_{wb}) \quad (3)$$

$$\Phi_t = 1/4(\Phi_{tr} + 2\Phi_{tm} + \Phi_{tl}) \quad (4)$$

where  $\Phi_{wt}$ ,  $\Phi_{wm}$  and  $\Phi_{wb}$  are the true plastic strain along the specimen width on the top, middle and bottom parts, respectively;  $\Phi_{tr}$ ,  $\Phi_{tm}$  and  $\Phi_{tl}$  are the true plastic strain along the specimen thickness on right, middle and left parts respectively.

## 3. Results and discussion

The influences of FSW parameters on joining performance of CP Ti butt joints are summarized in Fig. 1. The groove-like and inner cavity defects were detected when FSW was conducted at high welding speeds or low rotation rates, indicating that the generation of such defects was associated with the low thermal input and insufficient material flow. The overheating rough surface defects were observed when the high heat-input parameters, such as low welding speeds or high rotation rates, were used. Under appropriate adjustment of welding parameters, the joints without

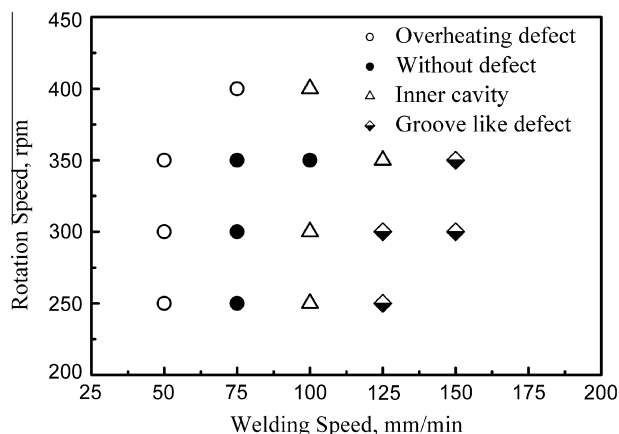


Fig. 1. Relationship between welding parameters and welding defects for FSW CP Ti.

defect were obtained within a narrow range of welding parameters. Similar phenomena was also observed in FSW of pure titanium lap joints in which the optimum welding parameter range is quite narrow. The groove-like and inner cavitation defect formed at low heat input while the overheating rough surface defect was formed when the high heat-input parameters were used [13,14].

The cross-sectional macrostructure of the FSW CP joint produced at 300 rpm and  $75 \text{ mm min}^{-1}$  is shown in Fig. 2a. The defect free SZ can be clearly observed due to its special grain structure. The microstructural details in the base material (BM) and different locations within the SZ are summarized in Fig. 2. The grains are colored in terms of the crystal direction. The low angle grain boundaries (LAGBs) were depicted as white lines and the high angle grain boundaries (HAGBs) as black lines. The BM was comprised of equiaxed  $\alpha$ -titanium and the average grain size is about  $42 \mu\text{m}$ . The EBSD maps showed that the grain structures which developed in the different locations of the SZ are broadly similar to each other. The dominant microstructural feature is fine and nearly equiaxed grains being surrounded by an irregular mixture of LAGBs and HAGBs. The grains typically contain almost no substructure and are mostly surrounded by HAGBs demonstrating a generation of full recrystallization in the SZ. The development of such a structural morphology can be attributed to the fact that the materials in the SZ has experienced significant plastic deformation during FSW. Dynamic recrystallization during FSW results in generation of fine and equiaxed grains in the SZ [3,4]. The average grain size in the SZ was determined to be about  $7 \mu\text{m}$  which was much less than that in the BM.

The BM has a typical rolling texture of  $\alpha$ -titanium with basal planes tilted about  $20\text{--}40^\circ$  from the normal direction towards the transverse direction (Fig. 2b). Similar to the previous reports [7–9], the strong  $P_1\{10\bar{1}0\}\{1\bar{2}10\}$  simple shear texture was observed in the different locations of the SZ (Figs. 2c–e). The  $P_1$  component rotates from retreating side (RS) to advancing side (AS) following the rotation of the shear direction across the SZ. The formation of such texture is mainly ascribed to the prismatic slip of  $\{10\bar{1}0\}\{1\bar{2}10\}$  caused by the simple shear deformation of the materials rotating around the stir tool during FSW. This also agrees with the commonly accepted theory that the prismatic slip is the dominate deformation mode in  $\alpha$ -titanium. Such a strong texture formed in the SZ may cause high Schmid factor for prismatic slip under tensile stress.

Vickers hardness profiles across the FSW joints produced at rotation rates of 250–350 rpm and a welding speed of  $75 \text{ mm min}^{-1}$  are plotted in Fig. 3. The SZ exhibited a hardness of about 180 HV, which was much higher than the average hardness of the BM (152 HV). The higher hardness in the SZ was attributed to the finer grain structures according to the Hall–Petch relationship in CP Ti [15,16]. Similar hardness distribution was also observed in the FSW of 3 mm thick CP Ti plates [8].

As stated in the experimental section, the top and bottom surfaces of the tensile samples were removed symmetrically to eliminate the influence of welding surfaces. This is beneficial to authentically reveal the influence of grain structure and texture on the deformation behavior in the SZ under transverse tensile stress. Tensile test showed that the ultimate tensile strength (UTS) of the joints produced at 250–350 rpm and  $75 \text{ mm min}^{-1}$  was in the range of 382–384 MPa, which are comparable to the UTS of the BM (Fig. 4a). The typical engineering stress–strain curve (Fig. 4b) showed that the engineering stress increased with increasing strain until a strain of approximately 0.1 (i.e. 10%) and then decreased continuously due to the development of necking. However, as typically shown in Fig. 5, distinctive plastic deformation extensively occurred in the SZ at the initial yielding stage during tensile test. The tensile samples finally fractured at the BM rather than the SZ. All the FSW joints failed in a similar way during tensile test.

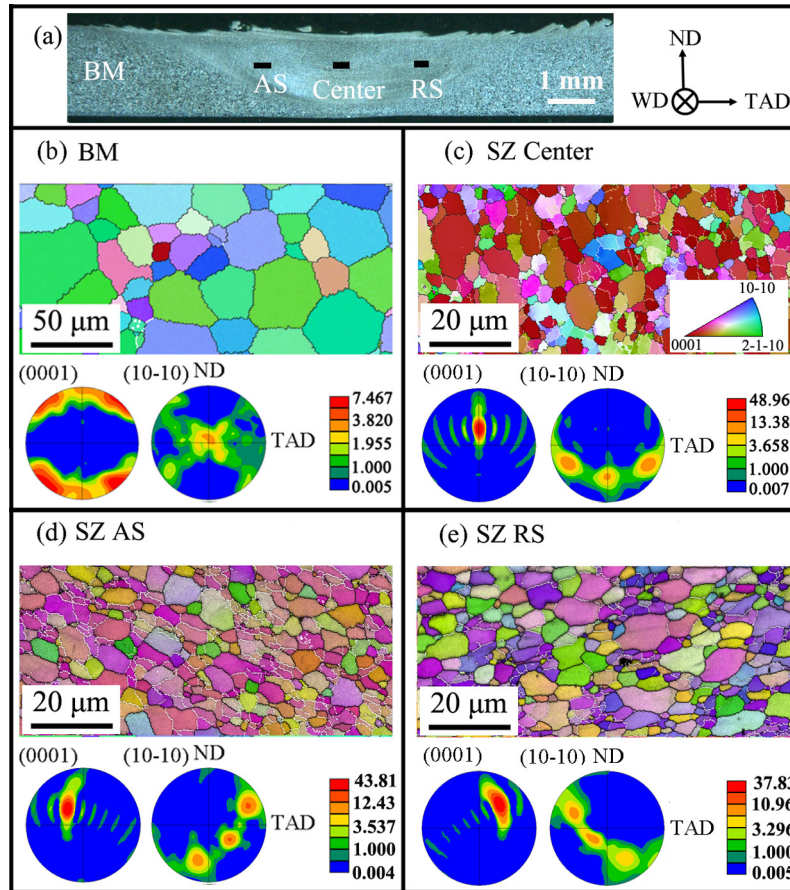


**Fig. 2.** Microstructural examination for sample welded at 300 rpm and 75 mm min<sup>-1</sup>: (a) cross-sectional macrostructural observation; EBSD results for undeformed sample in (b) BM, (c) SZ center, (d) advancing side within SZ and (e) retreating side within SZ (ND: normal direction, WD: welding direction, TAD: tensile axis direction which is parallel to transverse direction).

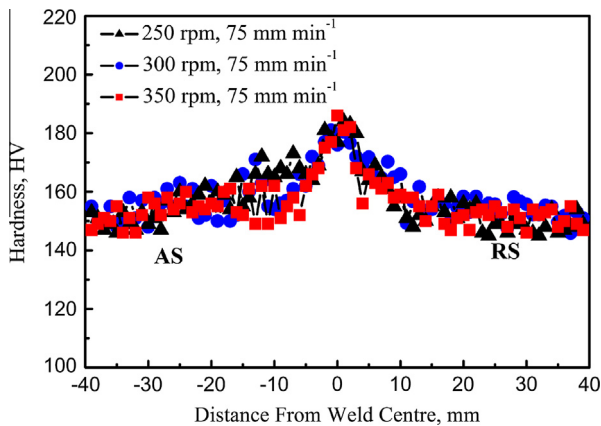


**Fig. 3.** Vickers hardness profiles across the FSW joints produced at 75 mm min<sup>-1</sup> and various tool rotation rates.

The cross-section overview of a typical tensile sample deformed to a strain of 0.1 (Fig. 6a) showed that the SZ center was thinner than other regions. Table 1 also showed a high  $r$  value in the BM and a low  $r$  value in the SZ center, indicating a dominant thickness strain occurred in the SZ center but a dominant width strain in the BM. It is also noted that the SZ center exhibited higher local elongation than the BM when the tensile sample was deformed to a strain of 0.1.

The microstructural evolution during tensile test in both the BM and the SZ center were investigated to clarify this special deforma-

tion behavior. There is not a significant variation in the grain structure for both the BM and the SZ after the sample was deformed to a strain of 0.1, except a small number of deformation twins appeared in the BM (Fig. 6b and c). The cause of extensive plastic deformation in the SZ at the initial yielding stage during tensile test cannot be traced to the grain structures but may be found in the special texture components in the SZ and the BM.

In the present work, the Schmid factor ( $\cos \varphi \cos \lambda$ ) for prismatic slip  $\{10\bar{1}0\}\langle 1\bar{2}10 \rangle$  which is the dominant deformation model for CP Ti was calculated based on the EBSD results, from which the  $\varphi$  and  $\lambda$  can be obtained. The calculation results showed that the Schmid factor for prismatic slip deformation in the AS, center, and RS regions within the SZ and the BM was mainly in the range of 0.31–0.36, 0.40–0.44, 0.30–0.35 and 0.19–0.25, respectively (Fig. 2). Because the Schmid factor of prismatic slip in the SZ center was higher than that in other regions and was much higher than that in the BM, it is possible that the remarkable plastic deformation occurred in the SZ center during the initial tensile deformation stage, even though the grain size was smaller in the SZ than in the BM. After the tensile sample was deformed to a strain of 0.1, the Schmid factor for prismatic slip deformation was reduced to 0.31–0.35 in the SZ center while it was increased to 0.26–0.31 in the BM (Fig. 6b and c). The difference of Schmid factor for prismatic slip deformation between the SZ and the BM was significantly reduced after tensile deformation. When tensile strain > 0.1, since the effect of grain size became more significant than Schmid factor, the local deformation in the SZ was restrained, and the tensile sample failed in the BM finally.

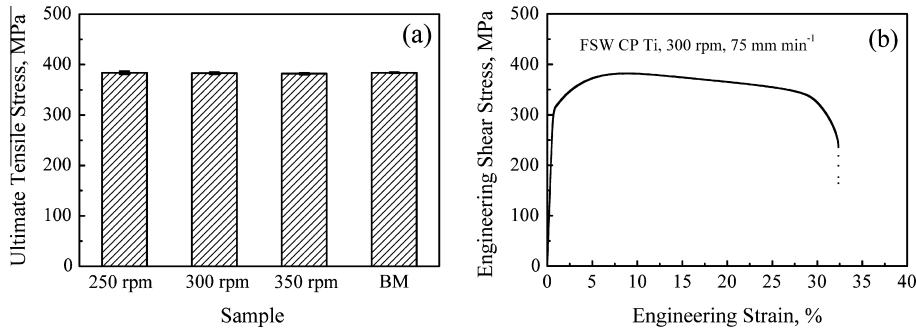


Fig. 4. Tensile results: (a) ultimate tensile stress summary; (b) stress vs. strain plot.

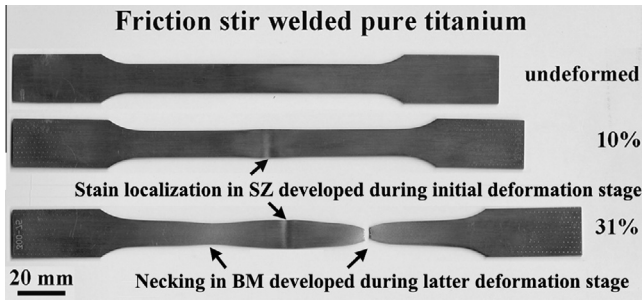


Fig. 5. Tensile samples deformed to different strains for FSW CP Ti welded at 300 rpm and 75 mm min<sup>-1</sup>.

Fig. 7 schematically illustrates the influence of texture on the materials flow during tensile test for FSW joints of CP Ti. The (0001) axis is aligned approximately parallel to the width direction of the tensile sample in the SZ center. Because the prismatic slip is the dominant slip system for CP Ti, the deformation of width direction is much more difficult than the deformation of thickness direction. This should be the reason why the high thickness strain was generated in the SZ center during tensile test.

In the BM, the degree between the (0001) axis and the thickness direction is less than 30°, much lower than that between the (0001) axis and the width direction of the tensile sample.

Table 1

True plastic strain along specimen width  $w$  ( $\Phi_w$ ) and thickness  $t$  ( $\Phi_t$ ), normal anisotropy ratio ( $r$ ), and calculated local elongation ( $El_{local}$ ) for BM and SZ center in tensile specimen with an elongation of 10%.

| Specimen  | ( $\Phi_w$ ) | ( $\Phi_t$ ) | $r$ ( $\Phi_w/\Phi_t$ ) | $El_{local}$ (%) |
|-----------|--------------|--------------|-------------------------|------------------|
| BM        | -0.084       | -0.015       | 5.60                    | 9.8              |
| SZ center | -0.028       | -0.102       | 0.27                    | 14.8             |

The deformation of thickness direction is more difficult than the deformation of width direction when prismatic slip is the dominated deformation. It is noted that the (0001) became sharpened after tensile deformation, indicating the occurrence of basal slip [14]. The prismatic slip generated mainly width strain, and the basal slip produced mainly thickness strain in the BM. The low  $r$  value at a strain of 0.1 indicated that the deformation in the BM was also dominated by prismatic slip.

#### 4. Practical implication

The present study showed that although the grains in the SZ are much finer than that in the BM, a distinctive plastic deformation still occurred within the SZ during the initial tensile deformation stage because the Schmid factor for prismatic slip in the SZ is much higher than the BM. The texture did not reduce the UTS because Schmid factor for prismatic slip in the SZ was reduced during

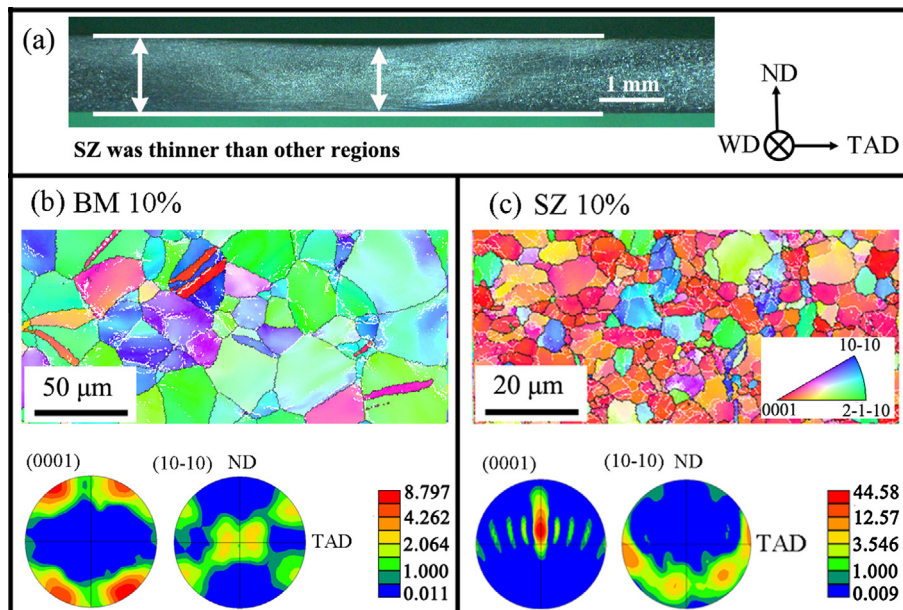


Fig. 6. Microstructural examination for deformed FSW joints welded at 300 rpm and 75 mm min<sup>-1</sup>: (a) optical profile along tensile axis; EBSD results for deformed sample in (b) BM and (c) SZ center.

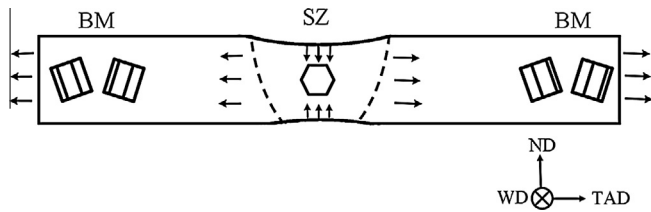


Fig. 7. Schematic illustration showing material flow on sample profile during tensile test.

tensile deformation. However, the premature yield deformation in the SZ reduces the load-carrying capacity estimation of the weld joints in practical strength design and may also have an adverse effect on the fatigue properties of the joints. Therefore, attention must be paid to the texture and strain localization in the SZ for FSW CP Ti. Developing other complex shaped tool to optimize the texture distribution in the SZ should be an effective method to improve the deformation resistance of the SZ.

## 5. Conclusions

A distinctive plastic deformation extensively occurred within the SZ during the initial tensile deformation stage because the Schmid factor for prismatic slip in the SZ is much higher than that in the BM. The difference of Schmid factor for prismatic slip deformation between the SZ and the BM was significantly reduced after tensile strain > 0.1, and the effect of grain size became more significant than Schmid factor. Therefore, the local deformation in the SZ which had a finer grain structure was restrained, and the tensile sample failed in the BM finally.

## Acknowledgment

One of the authors (F.C. Liu) wishes to acknowledge the support of FY 2014 JSPS Postdoctoral Fellowship for Foreign Researchers.

## References

- [1] W.B. Lee, C.Y. Lee, W.S. Chang, Y.M. Yeon, S.B. Jung, Microstructural investigation of friction stir welded pure titanium, *Mater. Lett.* 59 (2005) 3315–3318.
- [2] H. Fujii, Y. Sun, H. Kato, K. Nakata, Investigation of welding parameter dependent microstructure and mechanical properties in friction stir welded pure Ti joints, *Mater. Sci. Eng., A* 527 (2010) 3386–3391.
- [3] R.S. Mishra, Z.Y. Ma, Friction stir welding and processing, *Mater. Sci. Eng., R* 50 (2005) 1–78.
- [4] R. Nandan, T. DebRoy, H.K.D.H. Bhadeshia, Recent advances in friction Stir welding – process, weldment structure and properties, *Prog. Mater. Sci.* 53 (2008) 980–1023.
- [5] F.C. Liu, M.J. Tan, J. Liao, Z.Y. Ma, Q. Meng, K. Nakata, Microstructural evolution and superplastic behavior in friction stir processed Mg–Li–Al–Zn alloy, *J. Mater. Sci.* 48 (2013) 8539–8546.
- [6] F.C. Liu, Z.Y. Ma, M.J. Tan, Facilitating basal slip to increase deformation ability in Mg–Mn–Ce alloy by textural reconstruction using friction stir processing, *Metal. Mater. Trans. A* 44 (2013) 3947–3960.
- [7] Q. Yang, B.L. Xiao, D. Wang, M.Y. Zheng, K. Wu, Z.Y. Ma, Formation of long-period stacking ordered phase only within grains in Mg–Gd–Y–Zn–Zr casting by friction stir processing, *J. Alloys Comp.* 581 (2013) 585–589.
- [8] Y. Zhang, Y.S. Sato, H. Kokawa, S.H.C. Park, S. Hirano, Stir zone microstructure of commercial purity titanium friction stir welded using pcBN tool, *Mater. Sci. Eng., A* 488 (2008) 25–30.
- [9] S. Mironov, Y.S. Sato, H. Kokawa, Development of grain structure during friction stir welding of pure titanium, *Acta Mater.* 57 (2009) 4519–4528.
- [10] H. Liu, K. Nakata, N. Yamamoto, J. Liao, Grain orientation and texture evolution in pure titanium lap joint produced by friction stir welding, *Mater. Trans.* 51 (2010) 2063–2068.
- [11] R.W. Fonda, K.E. Knipling, Texture development in near- $\alpha$  Ti friction stir welds, *Acta Mater.* 58 (2010) 6452–6463.
- [12] K.E. Knipling, R.W. Fonda, Texture development in the stir zone of near- $\alpha$  titanium friction stir welds, *Scripta Mater.* 60 (2009) 1097–1100.
- [13] H. Liu, K. Nakata, N. Yamamoto, J. Liao, Friction stir welding of pure titanium lap joint, *Sci. Technol. Weld. Join.* 15 (2010) 428–432.
- [14] F.C. Liu, H. Liu, K. Nakata, N. Yamamoto, J. Liao, Investigation on friction stir welding parameter design for lap joining of pure titanium, in: *Proceeding of the 1st International Joint Symposium on Joining and Welding, Osaka, Japan, November 2013*, pp. 159–163.
- [15] P. Luo, D.T. McDonald, W. Xu, S. Palanisamy, M.S. Dargusch, K. Xia, A modified Hall–Petch relationship in ultrafine-grained titanium recycled from chips by equal channel angular pressing, *Scripta Mater.* 66 (2012) 785–788.
- [16] V.V. Stolyarov, Y.T. Zhu, T.C. Lowe, R.Z. Valiev, Microstructure and properties of pure Ti processed by ECAP and cold extrusion, *Mater. Sci. Eng., A* 303 (2001) 82–89.